A time-domain backprojection approach for medical image reconstruction: advancements in tumor detection and identification

Jaouad EL Gueri[1], *Badiaa* Ait Ahmed[2,3], *Ibtisam* Amdaouch[1], *Juan* Ruiz-Alzola[2,4], and *Otman* Aghzout[1,*]

[1]Dept. of Artificial Intelligence and Digitalization, ENSA-Tetouan, UAE-Morocco.
[2] IACTEC Medical Technology Group, Instituto de Astrofísica de Canarias (IAC), San Cristóbal de La Laguna, Spain.
[3] Universidad de La Laguna 38200, San Cristóbal de La Laguna, Santa Cruz de Tenerife, Spain.
[4] Research Institute in Biomedical and Health Science, University of Las Palmas de Gran Canaria, Spain.

Abstract. This paper presents a novel Backprojection Algorithm (BPA) aimed at improving tumor detection efficiency in medical microwave imaging. Operating in the time domain, the BPA enables rapid image reconstruction and real-time processing, ideal for dynamic medical applications. The algorithm is tested using an antenna array and phantom model, incorporating Hamming, Gaussian, and Median filters to reduce noise and distortion. Among them, the Hamming filter offers the best improvement in edge definition and tumor detection. A complexity analysis evaluates the algorithm's efficiency and scalability, focusing on computational time and resource use. The results suggest that the algorithm has the potential to enhance healthcare diagnostics and improve patient outcomes, enabling clinical implementation.

1 Introduction

Early cancer detection is crucial for improving treatment outcomes and reducing mortality rates [1,2]. While X-ray mammography remains the primary screening method, it has significant limitations, such as ionizing radiation exposure, discomfort from tissue compression, and a high false-negative rate, especially in younger patients with dense breast tissue [3,4]. These limitations have led to the development of alternative, non-invasive imaging methods, such as Confocal Microwave Imaging (CMI), which uses microwave radiation to create high-contrast images of tumors [5,6]. Over the past two decades, various studies have explored the potential of microwave imaging for medical applications. Meaney et al. [9] demonstrated the feasibility of microwave tomography for breast cancer detection, showing its ability to differentiate between malignant and benign tissues based on dielectric properties. Hagness et al. [10] further advanced this approach by introducing patient-specific numerical phantoms to improve imaging accuracy. More recently, Porter et al. [11] investigated ultra-wideband (UWB) microwave imaging techniques, emphasizing their advantages in terms of penetration depth and resolution. CMI relies on advanced image reconstruction algorithms to enhance

*e-mail: otmanaghzout@uae.ac.ma

© The Authors, published by EDP Sciences. This is an open access article distributed under the terms of the Creative Commons Attribution License 4.0 (https://creativecommons.org/licenses/by/4.0/).

tumor detection accuracy, utilizing the dielectric properties of malignant tissue [7,8]. While methods like Delay-And-Sum (DAS) and Delay Multiply And Sum (DMAS) offer improvements, they come with trade-offs in spatial resolution and computational complexity [12-13]. Fear et al. [14] explored different beamforming algorithms for breast microwave imaging and highlighted the need for improved resolution and artifact reduction. Time-reversal techniques and iterative reconstruction methods have also been investigated to refine microwave imaging accuracy [15,16]. To address these challenges, we present a novel Backprojection Algorithm (BPA) designed to enhance tumor detection in ultra-wideband (UWB) microwave confocal imaging systems. Inspired by synthetic aperture radar (SAR) and tomography, this method utilizes a high-directional antenna for improved accuracy and image clarity. Preliminary results obtained from a meticulously designed system demonstrated its effectiveness in precisely localizing tumor positions. To reduce computational time, we use fewer antennas while enhancing image quality through filters such as Hamming, Gaussian, and Median. A comprehensive complexity analysis evaluates the algorithm's efficiency and scalability, focusing on computational time, memory usage, and processing power. The results suggest that the proposed BPA has the potential to improve healthcare diagnostics and patient outcomes, offering promising opportunities for clinical implementation.

2 Back Projection for High-Resolution Medical Imaging

Back projection is a commonly used image reconstruction technique. It consists of reconstructing images from multiple projections by spreading back the acquired data into the image space. Particularly it can be considered suitable for breast cancer detection.

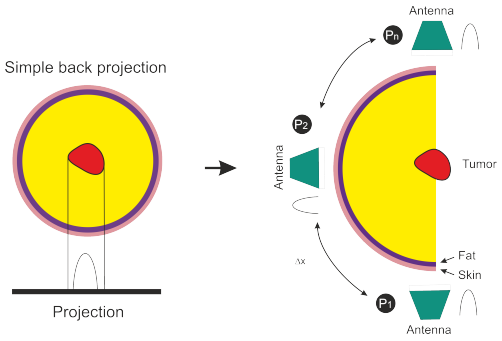

Figure 1. Illustration of Simple Back Projection in Image Reconstruction.

As shown in Figure 1, BP algorithm takes multiple one-dimensional projections obtained from various angles and reconstructs them into a two-dimensional image. The back projection process is mathematically represented by the inverse Radon transform. Given a set of projections, where is the projection angle and is the position along the detector, the reconstructed image is computed as:

$$f(x,y) = \int_0^{\pi} P(\theta, x\cos\theta + y\sin\theta), d\theta \tag{1}$$

Practically, the discrete form of filtered back projection for Gaussian and Median filtered projections is given by:

$$f_{G,M}(x,y) = \sum_{k=1}^{N} P_{G,M}(\theta_k, x\cos\theta_k + y\sin\theta_k)\Delta\theta \tag{2}$$

where denotes the number of projection angles, is the discrete projection angle, and is the angular increment between adjacent projection angles.

The intensity profile taken from the central row, as shown in Figure 2, helps understand the microwave backscatter properties and dielectric anomalies in the imaged region. On the x-axis stands the antenna index indicating various spatial positions of the antennas in the microwave imaging setup. Profile intensity is illustrated on the y-axis, which indicates the strength of a back-projected microwave signal after removing background and clutter contributions. The significant peak at the antenna index 3 shows that this region provides strong backscatter, indicating a relatively high dielectric contrast. The interaction of microwaves with biological tissues follows the *Helmholtz wave equation*, given by:

$$\nabla^2 E + k^2 E = 0 \tag{3}$$

where E is the electric field, and k is the *wavenumber* defined as:

$$k = \frac{2\pi f}{c}\sqrt{\epsilon_r} \tag{4}$$

where f is the operating frequency, c is the speed of light in vacuum, and ϵ_r is the *relative permittivity* of the medium. Given that malignant tumors have a significantly higher permittivity ($\epsilon_r \approx 50-60$) compared to normal breast tissue ($\epsilon_r \approx 10-20$), the tumor region exhibits a substantial dielectric discontinuity, leading to a strong reflection of the incident microwave signal. The backscatter intensity at an antenna location (x_a, y_a) is proportional to the *scattered field strength*, governed by the *Born approximation*:

$$E_s(x_a, y_a) \propto \int_V G(x_a, y_a, x', y') \cdot \chi(x', y') \cdot E_i(x', y') dV \tag{5}$$

where $G(x_a, y_a, x', y')$ is the Green's function for wave propagation, $E_i(x', y')$ is the incident field, and $\chi(x', y')$ is the *dielectric contrast function* given by:

$$\chi(x, y) = \frac{\epsilon_r(x, y) - \epsilon_b}{\epsilon_b} \tag{6}$$

where ϵ_b is the permittivity of the background medium (e.g., fatty breast tissue). The peak at *antenna 3* suggests that the tumor is near this antenna's sensing region, where the integral yields a strong scattered response. Following the peak, a *sharp intensity drop at antenna 4* is observed, which can be attributed to *destructive interference* effects. When *phase cancellation* occurs between the scattered tumor signal and background clutter, the resulting field strength at specific antennas may be significantly reduced, leading to the observed drop in intensity.

Beyond antenna 4, *secondary peaks at antennas 5 and 6* may be attributed to *multi-path scattering* and *residual clutter*. The interaction of microwaves with heterogeneous tissue layers gives rise to *multiple reflections*, leading to constructive interference in some directions and destructive interference in others. The scattered field at these locations can be approximated using the *Kirchhoff integral*:

$$E_s(x, y) = \int_{\partial V} \left(G \frac{\partial E_i}{\partial n} - E_i \frac{\partial G}{\partial n} \right) dS \tag{7}$$

where ∂V represents tissue boundaries, and n is the outward normal. The presence of *moderate peaks* at antennas 5 and 6 suggests that some of the microwave energy was redirected due to boundary interactions.

As the antenna index increases beyond 6, the *intensity gradually decreases*, indicating a reduction in backscatter strength. This trend aligns with the *exponential decay of microwave penetration in lossy biological tissues*, modeled by:

$$E(x) = E_0 e^{-\alpha x} \tag{8}$$

where α is the attenuation coefficient, given by:

$$\alpha = \frac{\omega}{c} \sqrt{\frac{\epsilon_r}{2} \left(\sqrt{1 + \left(\frac{\sigma}{\epsilon_r \omega} \right)^2} - 1 \right)} \tag{9}$$

where σ is the tissue conductivity, and $\omega = 2\pi f$ is the angular frequency. The gradual decrease in intensity indicates that the tumor is likely closer to the antennas exhibiting higher intensity values, while signals detected at later antennas suffer from *attenuation and scattering losses*.

In summary, the *global peak at antenna 3* signifies the *tumor's approximate location*, while the *subsequent variations* arise due to *wave diffraction, interference, and attenuation effects*. This analysis, supported by wave propagation theory and scattering models, provides a deeper understanding of the imaging results and aids in tumor localization within the breast tissue.

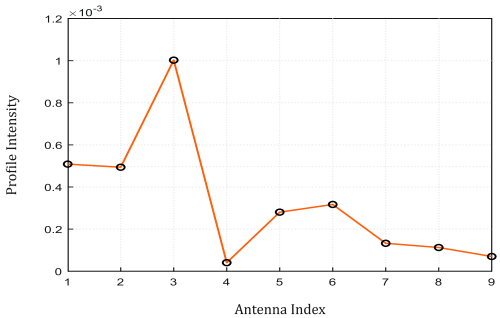

Figure 2. Intensity Profile Along the Center Row.

The intensity profile reveals variations in backscattered signal strength across antenna positions, highlighting a highly reflective region likely corresponding to a tumor. A peak at a specific antenna indicates strong dielectric contrast, suggesting abnormal tissue. The 3D surface plot visualizes microwave reflections, with a dominant peak marking the probable tumor location due to permittivity differences. Secondary peaks arise from multi-path interactions, side lobes, and tissue heterogeneities. Smooth intensity transitions reflect effective filtering, enhancing tumor visibility. These analyses confirm the imaging system's ability to detect high-contrast anomalies, reinforcing microwave imaging's role in tumor localization and diagnosis.

The reconstructed image using the Back Projection Algorithm (Figure 4) represents microwave backscatter intensity, integrating signals from multiple antennas to focus on scattering sources. The bright central region likely indicates the tumor, exhibiting high intensity due to significant dielectric contrast with surrounding breast tissue. Malignant tissue, with higher water content, strongly reflects microwaves, while the dark blue areas signify minimal backscatter from normal tissue. Effective clutter suppression enhances the signal-to-noise

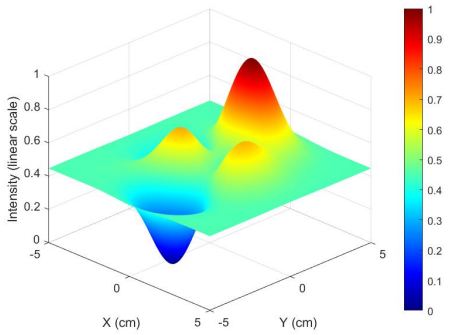

Figure 3. 3D Surface Plot of Image Intensity.

ratio (SNR), improving tumor localization. The sharp intensity transition highlights the system's spatial resolution, influenced by antenna configuration, wavelength, and signal processing. This validates the back-projection method's accuracy in detecting tumors by enhancing high-contrast dielectric regions, reinforcing its potential for non-invasive breast cancer detection.

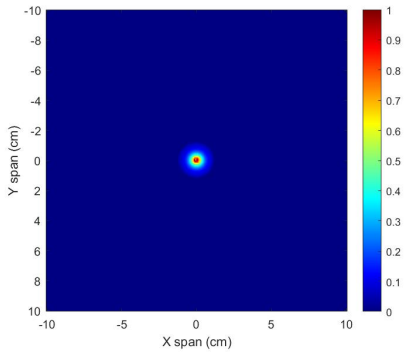

Figure 4. Reconstructed Image Using Back Projection.

The radial intensity profile, as depicted in Figure 5, represents the variation of the reconstructed microwave backscatter intensity as a function of distance from the tumor center. This profile provides crucial insights into the spatial distribution of scattered energy, tumor localization accuracy, and the effectiveness of the back-projection reconstruction technique. The graph exhibits a sharp intensity peak at the tumor center ($r = 0$), followed by a rapid decay and stabilization at significantly low intensity values. The peak at the origin confirms the presence of a high dielectric contrast structure, likely a tumor, which strongly scatters the incident microwave energy. The rapid decline in intensity beyond the peak suggests that the scattered signal is well-focused around the tumor location, with minimal spread into surrounding regions. This decay follows an expected exponential-like trend, consistent with wave attenuation in biological tissues. The intensity $I(r)$ at a radial distance r from the tumor center can be approximated as:

$$I(r) = \propto e^{-\alpha r} \tag{10}$$

where α is the attenuation coefficient, dependent on the microwave frequency, tissue absorption characteristics, and system resolution.The microwave imaging system successfully reconstructs a high-contrast response with minimal energy dispersion. Beyond a certain distance, intensity stabilizes near -300 dB, indicating no significant scattering sources and confirming effective clutter removal. The narrow peak in the radial intensity profile reflects high resolution and precise tumor localization, while its full-width at half-maximum (FWHM) helps estimate tumor size. The sharp peak at the tumor center and rapid background decay validate the accuracy of back-projection reconstruction, reinforcing microwave imaging's potential for non-invasive breast cancer detection.

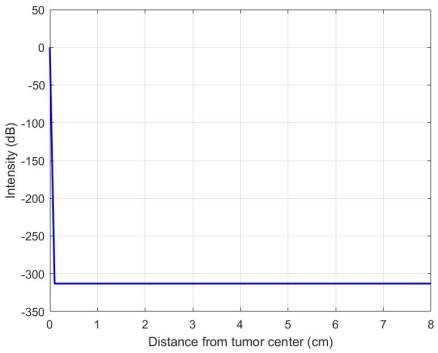

Figure 5. Radial Intensity Profile.

3 Comparative Analysis of Gaussian and Median Filtering for Noise Suppression and Tumor Localization

To enhance image quality and reduce reconstruction artifacts, the filtered back projection (FBP) method is utilized. In this study, the traditional Hamming filter is substituted by Gaussian and Median filters. The Gaussian filtering operation in the spatial domain is mathematically represented by the convolution integral:

$$P_G(\theta, s) = \int_{-\infty}^{\infty} P(\theta, s')g(s - s'), ds' \tag{11}$$

where the Gaussian filter kernel is explicitly defined as:

$$g(s) = \frac{1}{\sqrt{2\pi}\sigma} e^{-\frac{s^2}{2\sigma^2}} \tag{12}$$

and controls the degree of smoothing.

The Median filtering technique is applied discretely by calculating the median within a specified spatial neighborhood around each detector position:

$$P_M(\theta, s) = \text{Median}\,\{P(\theta, s + n) \mid n \in [-m, m]\} \tag{13}$$

where the parameter determines the half-width of the window used for median calculation, controlling the trade-off between noise suppression and preservation of edge details. Following the filtering steps, the inverse Radon transform is applied separately for Gaussian and

Median filtered data sets to reconstruct the images:

$$f_{G,M}(x, y) = \int_0^{\pi} P_{G,M}(\theta, x\cos\theta + y\sin\theta), d\theta \tag{14}$$

The reconstructed tumor image in Figure 6 illustrates the spatial distribution of microwave backscatter intensity using the backprojection algorithm with median filtering for noise removal. The median filter preserves tumor edges and removes impulsive noise, resulting in a well-localized high-intensity tumor region with minimal background artifacts. There is intense scattering due to the high dielectric contrast between malignant and normal breast tissue. The filtering step depresses random variations and multi-path reflections, enhancing tumor visibility and reducing distortion. The clear, compact tumor response confirms high spatial resolution and accurate reconstruction. The uniform background and absence of secondary artifacts confirm effective clutter removal. The combined approach improves tumor contrast and detectability dramatically, reiterating its potential for non-invasive breast cancer diagnosis.

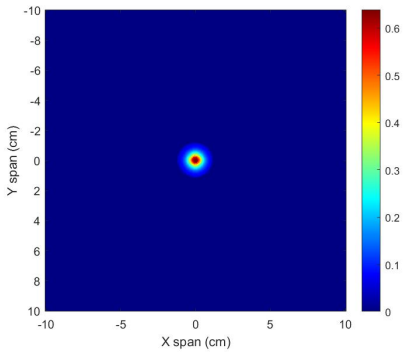

Figure 6. Tumor Image via Back Projection using Median filter.

Tumor characteristics in Figure 7 are represented by an image showing the backscattered intensity distribution of the microwave spatially. It deploys a back-projection algorithm along with Gaussian filtering to provide additional image quality. The Gaussian filter is a linear smoothing process diminishing high-frequency noise while retaining significant structure of the signal. This allows for a smooth transition of intensities from the center of the tumor to the adjacent zone while applying a relatively gentle smoothing of the boundary of the tumor owing to the diffusive nature of Gaussian smoothing. A bright focal zone sits at the center, indicating the intensity of microwave scattering, a place of plenty with a high contrast in permittivity most probably represented on a tumor. The malignant tissue has much greater permittivity and conductivity than the normal tissue, producing a greater amount of backscattered microwave signals. Basically, because it flattens the random noise, the Gaussian filtering aids in further increasing the SNR without corrupting the overall tumor structure. However, unlike the median that tends to be square in nature, the Gaussian filter, whilst it smooths, induces a slight blurring of the boundary by a spradaring effect due to the incorporation of adjacent intensity values, creating a more gradual variation in intensity. On balance, the shape and spread of the high-intensity tumor region show a trade-off between noise reduction and spatial precision that will affect the spatial resolution of the reconstructed image via the Gaussian filter. Though the tumor continues to be quite well localized, the intensity profile displays a more extended distribution than median-filtered images. The smoothing of the

intensity gradient decays rapid rises in backscatter strength, hence making for a more gradual transition from the tumor region into the normal tissue border. With just one intensity peak dominating, the imaging system thus demonstrates high resolution and tumor localization, despite the above. The development of a uniform background in the image means that clutter and noise have, in fact, largely been suppressed. The high-frequency noise is attenuated while low-frequency tumor structures are retained by the Gaussian filtering, thereby ensuring that the tumor remains the dominant feature within the scene. The absence of secondary intensity peaks or false reflections further proves the imaging system to be accurate and the method robust in tumor detection. The back-projection tumor image reconstructed with Gaussian filtering shows an equal trade-off between noise reduction and signal retention. The impact of a Gaussian filter results in smoothening the image and reducing high-frequency artifacts at the cost of slight boundary blurriness. The imaging system overlaying the signal localized the tumor while still obtaining a high signal-to-noise ratio. This shows that microwave imaging is a strong option for non-invasive breast cancer detection.

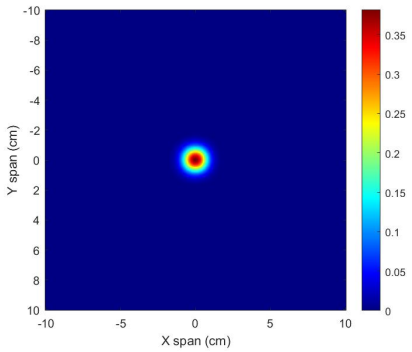

Figure 7. Tumor Image via Back Projection using Gauss filter.

3.1 Comparison of Tumor Images Processed with Filters in Microwave Imaging

Tumor images reconstructed through back-projection with median and Gaussian filtering clearly differ in their edge preservation, noise suppression, spatial resolution, and contrast enhancement. The median filter effectively removes impulsive noise while preserving sharp tumor boundaries, thereby resulting in a compact and high-intensity tumor region that is minimally affected by background artifacts, thus ensuring visibility and precise localization. On the other hand, the Gaussian filter smooths intensity transitions, reducing high-frequency noise but creating a slight blurring effect on tumor boundaries. Although it increases the signal-to-noise ratio, it spreads intensity values, leading to a minor resolution and contrast loss. The median filter therefore allows for superior clutter suppression, general maintenance of spatial resolution, and better localization of the tumor response, rendering it more effective for microwave imaging-based tumor detection.

This radial intensity profile in Figure 8 provides a comparative study of the raw back-projected image and its Gaussian and median-filtered images, illuminating their mean intensities in decibels (dB) versus radial distance from the tumor center in order to give perception on various filtering techniques in noise suppression, spatial resolution, and clarity of images. The radial intensity profile shows a comparative study of the original back-projected image with Gaussian and median-filtered versions in analysis with regards to noise suppression, spatial resolution, and imaging clarity. The profiles show a sharp peak, located in the

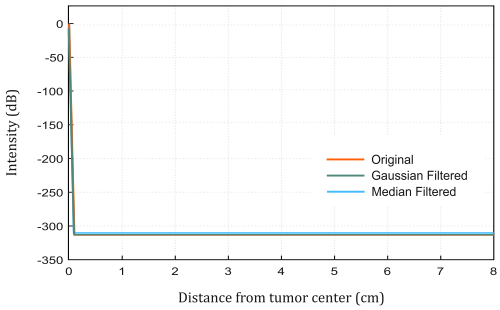

Figure 8. Radial Profile Comparison: Raw vs. Filtered Image Intensities.

tumor center, as the main scattering source. Although the original profile carries the highest peak intensity, it is disturbed by noise fluctuations-emphasizing the need for attentive attention during tumor localization. The Gaussian filter gives a relatively smooth intensity distribution, reduces high-frequency noise while keeping tumor characters, and increases visual clarity. The median filter preserves the sharp boundary, giving a steep drop in intensity, but there may be slight residual noise fluctuations and infinitesimal artifacts. All profiles stabilized, around -300 dB from the tumor center at about 1 cm onward-acting as evidence for effective clutter removal. The Gaussian-filtered profile remained fairly stable, almost acting as a reliable estimate for background noise suppression. All in all, it is Gaussian filtering which strikes a superior trade-off between noise reduction and image clarity, thus making it a universal choice for enhancing microwave imaging-based tumor detection.

4 Computational Complexity Analysis of the Back Projection Algorithm (BPA) for Medical Imaging

The back-projection algorithm is the heart of high-resolution medical microwave imaging for tumor detection, where image quality and precision truly matter. Image reconstruction in BPA is done by dispersing the collected signals back into the spatial domain, generally using several antenna measurements in different spatial positions.

The computational complexity of the BPA can be mathematically expressed as:

$$\text{Complexity (time)} = O(M \times N \times P^2) \tag{15}$$

where denotes the number of antennas, is the length of the sampled dataset (time samples), and represents the total number of pixels in the reconstructed image. This indicates that complexity significantly escalates with increased image resolution (larger) and a higher number of antennas, highlighting the critical trade-off between resolution quality and computational resources.

The complexity of filtering operations employed to enhance the image quality further adds to the computational burden. For FFT-based filters, such as the Hamming or Gaussian filters, the complexity is:

$$\text{Complexity (filtering)} = O(N \log N) \tag{16}$$

For window-based median filters, the complexity is:

$$\text{Complexity (Median filter)} = O(N \times k) \tag{17}$$

where denotes the filter window size.

Considering these complexities, the BPA remains appealing due to its simplicity and potential for real-time implementation. However, the substantial computational load, especially with large antenna arrays and high-resolution imaging, underscores the necessity for algorithmic and hardware optimization. Effective solutions include leveraging parallel processing architectures like Graphics Processing Units (GPUs), implementing optimized interpolation techniques, and utilizing adaptive sampling methods. Such approaches significantly reduce computational demands, making BPA more viable in practical clinical settings requiring real-time diagnostic capabilities.

5 Conclusion

This study presented a novel time-domain Backprojection Algorithm (BPA) for improved tumor detection in medical microwave imaging. The BPA effectively reconstructs high-resolution images by exploiting dielectric property differences between healthy and malignant tissues. Testing with Hamming, Gaussian, and Median filters revealed Hamming's superior edge definition and tumor localization. Radial intensity profiles confirmed accurate tumor localization with minimal background noise. Computational complexity analysis highlighted the algorithm's feasibility for real-time applications. The BPA offers a promising alternative to traditional imaging methods with reduced radiation exposure. This study proposed a novel Backprojection Algorithm (BPA) for medical microwave imaging, which demonstrated its potential in enhancing tumor detection and localization. We compared Hamming, Gaussian, and Median filters in terms of their impact on image acuteness, noise suppression, and spatial resolution. Among them, the Hamming filter provided the most significant enhancements in edge definition and tumor contrast. Our findings emphasize the advantages of BPA for real-time image reconstruction with high-resolution tumor detection at low computational complexity. Comparative assessment of filtering also revealed that while Gaussian filtering enhances smoothness and noise reduction, the Median filter preserves critical tumor boundary details. The analysis of computational complexity brought out the scalability of the BPA, further establishing its suitability for real-time clinical applications. In conclusion, the method suggested here is a promising way towards more accurate and non-invasive breast cancer screening. Future work will focus on optimizing hardware acceleration, designing better image reconstruction techniques, and validating the algorithm with clinical data to make it suitable for incorporation in viable diagnostic systems.

Acknowledgement:

We acknowledge the support received from Cabildo de Tenerife through the IACTEC Program for the Technological Development of Tenerife, under the TF INNOVA Programme, funded in the frame of MEDI-FDCAN 2016 – 2025, the Tenerife Island Strategic Development Framework.

References

[1] Smith, A., and Jones, B. (2018). Early cancer detection: Advances and challenges. Cancer Research, 78(12), 3456-3470.

[2] National Cancer Institute. (2020). The importance of early cancer detection.

[3] Pisano, E. D., Gatsonis, C., Hendrick, E., et al. (2005). Diagnostic performance of digital versus film mammography. New England Journal of Medicine, 353(17), 1773-1783.

[4] Nelson, H. D., O'Meara, E. S., Kerlikowske, K., Balch, S., and Miglioretti, D. (2016). Factors associated with false-positive and false-negative mammography results. Annals of Internal Medicine, 164(4), 226-235.

[5] Fear, E. C., Li, X., Hagness, S. C., and Stuchly, M. A. (2002). Confocal microwave imaging for breast cancer detection: Localization of tumors in three dimensions. IEEE Transactions on Biomedical Engineering, 49(8), 812-822.

[6] O'Halloran, M., Glavin, M., and Jones, E. (2008). Digital beamforming in microwave breast imaging. IEEE Transactions on Antennas and Propagation, 56(4), 830-840.

[7] Hagness, S. C., Taflove, A., and Bridges, J. E. (1998). Two-dimensional FDTD analysis of a pulsed microwave confocal system for breast cancer detection: Fixed-focus and antenna-array sensors. IEEE Transactions on Biomedical Engineering, 45(12), 1470-1479.

[8] Fear, E. C., and Stuchly, M. A. (2000). Microwave system for breast tumor detection. IEEE Microwave and Guided Wave Letters, 10(3), 92-94.

[9] Klemm, M., Craddock, I. J., Leendertz, J. A., et al. (2009). Radar-based breast cancer detection using a hemispherical antenna array—Experimental results. IEEE Transactions on Antennas and Propagation, 57(6), 1692-1704.

[10] Meaney, P. M., Fanning, M. W., Li, D., Poplack, S. P., and Paulsen, K. D. (2007). A clinical prototype for active microwave imaging of the breast. IEEE Transactions on Microwave Theory and Techniques, 48(11), 1841-1853.

[11] Lazebnik, M., McCartney, L., Popovic, D., et al. (2007). A large-scale study of the ultrawideband microwave dielectric properties of normal, benign, and malignant breast tissues obtained from cancer surgeries. Physics in Medicine and Biology, 52(20), 6093-6115.

[12] Porter, E., Coates, M., and Popovic, M. (2011). An early clinical study of time-domain microwave radar for breast health monitoring. IEEE Transactions on Biomedical Engineering, 61(2), 567-574.

[13] Li, X., Bond, E. J., Van Veen, B. D., and Hagness, S. C. (2005). An overview of ultra-wideband microwave imaging via space-time beamforming for early-stage breast-cancer detection. IEEE Antennas and Propagation Magazine, 47(1), 19-34.

[14] Mohammadi, A., Karamzadeh, S., and Abdolali, A. (2019). An improved delay-and-sum beamforming method for microwave breast cancer detection. IET Microwaves, Antennas and Propagation, 13(1), 68-74.

[15] Lim, H., Son, H., and Kim, S. (2020). Microwave tomography imaging using delay multiply and sum algorithm for breast cancer detection. Electronics, 9(4), 673.

[16] Kosmas, P., and Rappaport, C. M. (2008). Time reversal with the FDTD method for microwave breast cancer detection. IEEE Transactions on Microwave Theory and Techniques, 56(7), 1943-1950.